

2021-12-14

Soil erosion and sediment transport in Tanzania: Part I sediment source tracing in three neighbouring river catchments

Wynants, Maarten

<http://hdl.handle.net/10026.1/18469>


10.1002/esp.5217

Earth Surface Processes and Landforms

Wiley

All content in PEARL is protected by copyright law. Author manuscripts are made available in accordance with publisher policies. Please cite only the published version using the details provided on the item record or document. In the absence of an open licence (e.g. Creative Commons), permissions for further reuse of content should be sought from the publisher or author.

Soil erosion and sediment transport in Tanzania: Part I – sediment source tracing in three neighbouring river catchments

Maarten Wynants¹  | Linus Munishi² | Kelvin Mtei² | Samuel Bodé³ | Aloyce Patrick² | Alex Taylor¹ | David Gilvear¹ | Patrick Ndakidemi² | William H. Blake¹ | Pascal Boeckx³

¹School of Geography, Earth and Environmental Sciences, University of Plymouth, Plymouth, UK

²Nelson Mandela African Institution of Science and Technology, Arusha, Tanzania

³Isotope Bioscience Laboratory – ISOFYS, Ghent University, Ghent, Belgium

Correspondence

Maarten Wynants, School of Geography, Earth and Environmental Sciences, University of Plymouth, Portland Square, Drake Circus, Plymouth, PL4 8AA, UK.

Email: maarten.wynants@plymouth.ac.uk

Funding information

European Commission (Horizon 2020 IMIXSED project ID), Grant/Award Number: 644320; University of Plymouth, Faculty of Science and Engineering, PhD Scholarship; UK Natural Environment Research Council, Grant/Award Number: NE/R009309/1; Research Council UK Global Challenges Research Fund (GCRF), Grant/Award Number: NE/P015603/1

Abstract

Water bodies in Tanzania are experiencing increased siltation, which is threatening water quality, ecosystem health, and livelihood security in the region. This phenomenon is caused by increasing rates of upstream soil erosion and downstream sediment transport. However, a lack of knowledge on the contributions from different catchment zones, land-use types, and dominant erosion processes, to the transported sediment is undermining the mitigation of soil degradation at the source of the problem. In this context, complementary sediment source tracing techniques were applied in three Tanzanian river systems to further the understanding of the complex dynamics of soil erosion and sediment transport in the region. Analysis of the geochemical and biochemical fingerprints revealed a highly complex and variable soil system that could be grouped in distinct classes. These soil classes were unmixed against riverine sediment fingerprints using the Bayesian MixSIAR model, yielding proportionate source contributions for each catchment. This sediment source tracing indicated that hillslope erosion on the open rangelands and maize croplands in the mid-zone contributed over 75% of the transported sediment load in all three river systems during the sampling time-period. By integrating geochemical and biochemical fingerprints in sediment source tracing techniques, this study demonstrated links between land use, soil erosion and downstream sediment transport in Tanzania. This evidence can guide land managers in designing targeted interventions that safeguard both soil health and water quality.

KEYWORDS

geochemical fingerprinting, sediment tracing, compound specific stable isotope analysis, Bayesian mixing models, (sub)surface erosion, land use, East Africa, river catchment

1 | INTRODUCTION

River catchments in Tanzania have some of the highest sediment yields of sub-Saharan Africa, linked in part to a distinct topography and the semi-arid climate (Vanmaercke et al., 2014), but also to the effects of increasing land-use pressures (Borrelli et al., 2017; Wynants et al., 2019). The loss of permanent vegetation through deforestation,

agricultural expansion and overgrazing is driving accelerating rates of erosion, which is causing a rapid depletion of soil resources, threatening food, water and livelihood security in the region (Fenta et al., 2020; Maitima et al., 2009). Furthermore, these processes are potentially amplified by natural rainfall variations (Ngecu & Mathu, 1999; Wynants et al., 2020) and projected increases in extreme climatic events (Borrelli et al., 2020). While soil resources are

This is an open access article under the terms of the Creative Commons Attribution License, which permits use, distribution and reproduction in any medium, provided the original work is properly cited.

© 2021 The Authors. *Earth Surface Processes and Landforms* published by John Wiley & Sons Ltd.

progressively being depleted, the Tanzanian population and their demand for the services the soil provides is increasing (FAO, 2019; UNDESA, 2017). Continued loss of productivity and arable land would be catastrophic for the agricultural sector in Tanzania, which currently employs about 75% of the working population, underpins the economy, and provides the basic caloric uptake for the majority of its inhabitants (FAO, 2019; Salami et al., 2010; Sanchez, 2002; Tengberg & Stocking, 1997). Besides these on-site impacts, increased downstream sediment transport also has major detrimental effects on aquatic ecosystems, water quality and energy security (Amasi et al., 2021; Dutton et al., 2019; Olago & Odada, 2007). There is an urgent need for science-based land- and water-management strategies in Tanzania to achieve sustainable intensification of agro-pastoral production and protect soil resources. However, a lacuna in environmental data and a lack of understanding on the complex dynamics of increased soil erosion and sediment transport in semi-arid East Africa impedes the development and application of sustainable land- and water-management plans (Blake et al., 2018b; Kelly et al., 2020).

In this context, sediment source tracing techniques are valuable tools for filling knowledge gaps and elucidating processes of soil erosion and sediment transport (Collins et al., 2017; Walling, 2013). Soils and ecosystems co-evolve through a mutual interdependence on the balance between soil erosion and soil production through weathering (Lowdermilk, 1953). Differences in geology, climate, ecosystem structure, land use, and pedogenetic processes, give the resulting soils a characteristic geochemical and biochemical composition. Geochemical and biochemical fingerprinting can be used for grouping potential sources into different catchment zones, land-use types and soil depths (Gibbs, 2008; Motha et al., 2002; Reiffarth et al., 2016). Surface and subsurface erosion processes can detach soil and regolith particles, which are transported downstream from different catchment areas by hydrological processes as a mixture of sediment particles (Fryirs, 2013; Hoffmann, 2015; Kitch et al., 2019). During detachment, transport and deposition, sediment particles are, however, subject to sorting effects depending on their particle size (Lacey et al., 2017). Moreover, during these processes, tracers are also potentially subject to chemical alterations (Belmont et al., 2014). The biochemical and geochemical composition of riverine sediments thus depends on the relative contributions of different sources, their physical and chemical properties, and the transport dynamics in the river system (Haddadchi et al., 2013; Walling, 2013; Walling & Woodward, 1995). Integrating multivariate source and mixture fingerprints within Bayesian mixing models (BMMs) allows a proportional attribution of soil sources to downstream sediment (Blake et al., 2018a; Collins et al., 2010, 2017; Cooper et al., 2015). With respect to good practice, sediment source tracing can be a powerful tool for investigating the contributions of different catchment zones, erosion processes and land-use types to the sediment (Alewell et al., 2016; Blake et al., 2012; Owens et al., 2016).

By using complementary sediment source tracing techniques, this study aims to assess the dominant sources of transported sediment in Tanzanian river systems distinguishing between catchment zones, dominant land-use types and erosional processes. This is done by fingerprinting potential source material and river sediment in three neighbouring Tanzanian catchments using elemental geochemistry and the $\delta^{13}\text{C}$ signature of plant-derived, long-chain (> C22), saturated fatty acids (FAs). The importance of land use, catchment zone, and

erosion processes to the sediment fluxes is quantified using BMMs. Estimations of source zone contributions to riverine sediment are particularly valuable for designing targeted management interventions to maintain both soil health and water quality. This article is the first part of an article pair, wherein the second article studies the changes in soil erosion and sediment transport in the region over the past 120 years (Wynants et al., 2021).

2 | MATERIAL AND METHODS

The raw dataset, model inputs, model build, and model outputs are available as open access at <https://doi.org/10.24382/9xmf-7e88>.

2.1 | Study area

Sedimentation rates in Lake Manyara have increased significantly over the past 120 years (Wynants et al., 2020), which threatens the ecosystem health and services of this National Park and UNESCO Man and Biosphere Reserve (Janssens de Bisthoven et al., 2020). Previous research of Wynants et al. (2020) attributed the observed increase in sedimentation in Lake Manyara in the past decades mainly to increased sediment delivery from the Makuyuni River. The Makuyuni system is spatially and hydrologically complex (Figure 1 and Supporting Information Figure S1), wherein its northern tributaries drain the Monduli, Lesimingore and Lepurko volcanic highlands, dominated by Andosols and Leptosols (Nachtergaele et al., 2008). They subsequently flow to the middle elevation zone, dominated by Chernozems, and converge with each other and with the southern tributaries further down in the drier Maasai steppe, from which the main river flows towards Lake Manyara.

The rainfall is seasonal and characterized by a bimodal rainy season with a short peak from November to December and a longer peak from February to May. Moreover, the rainfall is spatially variable in the catchment (Figure S1), with higher levels of annual precipitation at the higher elevations (Nicholson, 1996; Prins & Loth, 1988). Connectivity between tributaries is often not accomplished due to localized precipitation, loss of runoff water by infiltration and evapotranspiration, diverging flows, and the presence of sinks, such as reservoirs, between upland areas and the main river network (Guzha et al., 2018; Jacobs et al., 2018). This gives the Makuyuni a typical ephemeral character, with low or no flow in the drier periods and a high discharge during and after rainstorms. During these peak flows, the river can also spill into its connected flood plains. The conjunction of these climatic and hydrological processes also creates a natural vegetation continuum from drier lowland rangelands to upland forests (Prins & Loth, 1988; Wynants et al., 2018). Open savanna rangelands, bushlands, agriculture, and bare land dominate the land cover (Table 1). Smaller pockets of forest and wetland vegetation are confined to the uplands and floodplains, respectively. However, a combination of unsustainable land-cover changes and a natural high vulnerability to soil erosion resulted in a marked increase in surface erosion, gully incision and land degradation in the area (Blake et al., 2018b; Kiunsi & Meadows, 2006; Maerker et al., 2015; Wynants et al., 2018). Therefore, three sub-catchments (Figure 1 and Table 1) were selected for a detailed investigation into the sources of transported sediment: Nanja,

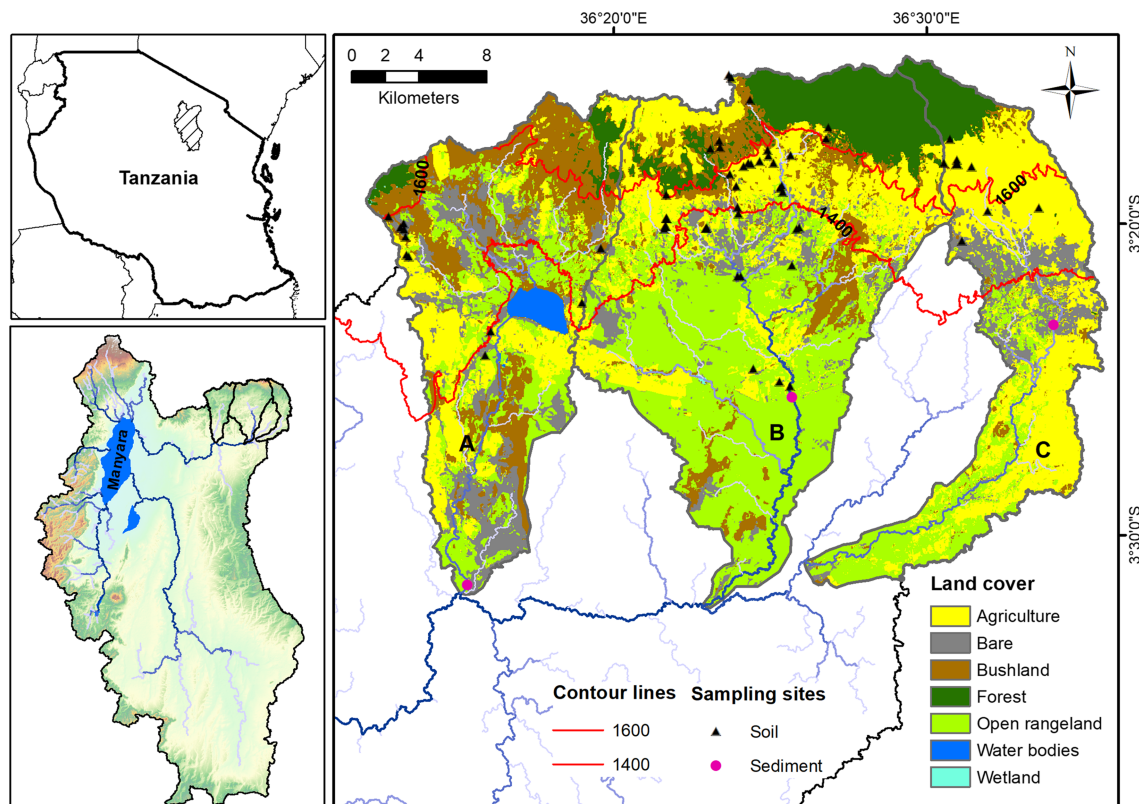


FIGURE 1 Location of: A, Nanja sub-catchment; B, Ardai sub-catchment; C, Musa sub-catchment depicting the sampling locations of source soils (black triangles) and riverine sediment (pink circles). The 1400 and 1600 indicate the proximate borders between the low-zone (< 1400), mid-zone (1400–1600) and up-zone (> 1600) of the catchment. The land cover of the catchments is given, as well as its geographical context within the Lake Manyara system and in Tanzania [Color figure can be viewed at wileyonlinelibrary.com]

TABLE 1 Characteristics of the studied river catchments and an overview of the amount and types of samples taken

River system	Ardai	Nanja	Musa
<i>Catchment characteristics</i>			
Catchment area (km ²)	390	240	182
Elevation range (m)	1266–2658	1165–2124	1351–2642
Agriculture (%)	25.7	22.3	53.3
Bare (%)	7.1	19.2	14.2
Bushland (%)	11.4	29.0	2.8
Forest (%)	12.6	3.3	7.5
Open rangeland (%)	43.1	23.8	22.2
Wetlands (%)	0.1	0.0	0.0
Water bodies (%)	0.0	2.5	0.0
<i>Sampling locations</i>			
Suspended sediment	8	–	3
Deposited sediment	9	7	9
Surface soil	90	49	48
Subsurface soil	32	17	15

Ardai and Musa. Due to their variability in soil types, geology, rainfall, altitude and dominant land use, both within and between the three catchments, they are a natural microcosm of the wider northern Tanzanian landscape, allowing a representable study of soil erosion and sediment transport in the region.

The dominant land-use groups (Table 1) were obtained from a previous land-cover reconstruction of the area by Wynants (2018),

combined with ground observations made during fieldwork. The catchment was grouped into three approximate zones wherein the up-zone (> 1600 m) is generally characterized by younger soils developed on volcanic rocks, steeper slopes and higher rainfall. The low-zone (< 1400 m) is generally characterized by sandier soils developed on older metamorphic rocks, lower slopes and lower rainfall. The mid-zone (1400 m–1600 m) is an intermediate zone with often deeply

weathered soils, medium to steep slopes and variable rainfall levels. The main distinction between erosion process was made between surface erosion, consisting of rill and interrill erosion, and subsurface erosion, consisting of gully and riverbank erosion. Photographs of the erosion features in the study area can be found in the discussion.

2.2 | Sampling strategy

Respectively 122, 66 and 63 soil samples were taken from 26, 8 and 8 sites in the Ardai, Nanja and Musa sub-catchments (Figure 1 and Table 1). Sampling sites in each sub-catchment were selected to account for the variation in the three levels of interest: land use, catchment zone and erosion process. The specific sampling locations were further subject to accessibility, necessary permits and safety. Surface soils were sampled by taking 5–10 integrated soil samples (five scoops of top 3 cm soils per sample) along a 100 m spatial transect. Subsurface samples were sampled from gully banks and riverbanks in the three catchment zones. A clear distinction between gullies and the river network was not made due to the gradual transition and ephemeral character of the entire system. Gully banks were sampled by grouping 10 scoops at the same depth into one composite sample. The depth of the composite gully samples was taken just above the active scouring face and was therefore dependent on the gully depth. In the riverbanks and deeper gullies, composite samples were also taken from different depths using intervals of c. 1 m to test for vertical differences in the tracer concentrations.

Riverine sediment was collected in three sampling campaigns for Ardai (two dry seasons and one rainy season), two sampling events for Nanja (two dry seasons), and two sampling events for Musa (one dry season and one rainy season) over a 2-year period, attempting to integrate as much seasonal and interannual differences in the sediment fingerprint as logistically possible. If the rivers were dry or in low flow, deposited sediment (DS) was collected by taking 5–10 composite samples, each composed of 10 scoops of material from depositional features with clear indication of deposition by water. DS samples were taken over a length of about 200 m to account for random spatial variability in riverine sediment deposition (Gellis & Noe, 2013; Wilkinson et al., 2013). Since the sampling of DS took place in the dry season, it was assumed that the DS samples integrated the sediment from multiple smaller flow events (Smith & Dragovich, 2008). If the rivers were in high flow during the wet season, suspended sediment (SS) samples were taken by collecting 3–5 bottles of 1.5 L river water and letting it settle. Due to the non-quantitative approach to SS collection, no estimations of SS load could be made. In the Ardai system, sediment was collected from two high flow events (SS) and two times at no flow in the dry season (DS). The Musa system was sampled in one flow event (SS) and two times in the dry season (DS). The Nanja outlet was not reachable in the wet season and was therefore only sampled two times in the dry season using the DS approach.

2.3 | Laboratory analysis

Sediment and soil samples were either freeze-dried or oven-dried at 40°C and subsequently disintegrated using a mortar and pestle.

Samples were analysed for major and minor element geochemistry by wavelength dispersive X-ray fluorescence (WD-XRF; OMNIAN application, Axios Max, Malvern PANalytical, Malvern, UK) as pressed pellets. Prior to analysis all samples were sieved to < 63 µm to limit particle size effects (Lacey et al., 2017; Motha et al., 2002) and because of the general focus on the detrimental fine sediment (Walling, 2013). The sieved < 63 µm fraction was further homogenized by milling it for 20 min at 300 rpm in order to reduce shadowing effects and preferential analysis of finer particles (Willis et al., 2011). Measurements were validated using stream sediment certified reference material (GBW07318, LGC, Middlesex, UK). Triplicates were made of randomly selected samples to assess repeatability of the method. Instrument drift was assessed following internal quality control procedures using a multi-element glass sample. Only those elements returning measurements above the limit of detection for > 75% of the samples and with triplicate variability < 5% were used in further analysis.

Compound specific stable isotope analysis (CSIA) of FAs was performed following the methodology described by Upadhayay et al. (2018). Due to the high labour and financial costs of CSIA, only soil and sediment samples from the Ardai sub-catchment were selected for analysis. A recovery standard (C17:0 FA, no natural occurrence) was added before lipid extraction to evaluate FA extraction efficiency. Lipids were extracted with accelerated solvent extraction (ASE 350; Dionex, Thermo Scientific, San Jose, California, US) using dichloromethane–methanol (9:1, v/v) at 100°C and 1.3×10^7 Pa for 5 min in three cycles (30 mL cells, 60% flush volume). The volume of total lipid extract was reduced by evaporation at reduced pressure and neutral and acidic compounds were separated using solid-phase extraction on aminopropyl-bonded silica gel columns. The acid fraction was methylated with methanolic HCl of known carbon isotopic composition ($\delta^{13}\text{C} = -40.78 \pm 0.33\%$) and ethylated C20:0 FA was added afterwards as an internal standard. Fatty acid methyl esters (FAME) concentrations were measured using gas chromatography with flame ionization detection (GC-FID; TRACE GC, Thermo Scientific, Waltham, MA, USA). The solvent volume was adapted to obtain ideal concentration for isotope determination with capillary gas chromatography-combustion-isotope ratio mass spectrometry (GC-C-IRMS; TRACE GC Ultra interfaced via a GC/C III to DeltaPLUS XP, Thermo Scientific). Isotope ratios were expressed as $\delta^{13}\text{C}$ values in per mill relative to the VPDB standard. An in-house prepared Schimmelman FAME mix reference (C20–C30 FAs), traceable to IAEA-CH6, was injected every six samples for $\delta^{13}\text{C}$ calibration. The $\delta^{13}\text{C}$ values of the analysed FAME were corrected for the methanol group that was added during derivation using the internal standard measurements. The short-chained $\delta^{13}\text{C}$ -FA C16–C21 were omitted out of the further analysis because they are more susceptible to degradation and are predominately produced by microorganisms (Upadhayay et al., 2017).

On a selection of soil samples from representative locations over the catchment, the organic matter (OM) content and aggregate stability (AS) was estimated. OM was estimated using loss of ignition (LOI), wherein the percentage of mass lost after 24 h at 450°C was calculated (Heiri et al., 2001). AS was calculated using laboratory rainfall simulation on a 45 mm/h intensity with a mean drop size of 580 µm. A mean rainfall simulation survival index (RSSI) was calculated based on the number of aggregates surviving at 5, 10, 15 and 20 min during the test (Ternan et al., 1996).

2.4 | Data analysis

2.4.1 | Source grouping

Source grouping based solely on geospatial information might lead to grouping samples together with very different fingerprints, which would reduce the model efficacy. Vice versa, grouping samples solely based on unsupervised statistical techniques might lead to soil clusters that are not relevant from a geospatial and ultimate a land management point of view. Therefore, the source grouping in this study was done using a combination of geospatial analysis (GA) and unsupervised cluster analysis (CA) that were integrated using principal component analysis (PCA).

The first step in the source grouping was to perform a CA of the soil samples for each sub-catchment using the unsupervised 'K-means' method of Forgy (1965), where the only expert input is the number of cluster numbers, and the outcomes are soil groups solely based on the variation in the multivariate fingerprint. The number of clusters was selected based on the elbow technique, wherein the number of clusters was chosen so that adding another cluster did not reduce the intra-cluster variance significantly (Kassambara, 2017). This information was combined with expert-set expectations of source delineation based on the geospatial information, but also on model feedback. The highest number of clusters was in all cases taken at seven because the MixSIAR model can only produce reliable unmixing results up to seven sources (Stock et al., 2018).

The second step of the source grouping was to perform a PCA of the multivariate source samples for each sub-catchment to reduce the dimensionality and plot the geochemical or biochemical fingerprints on a biplot (Hardy et al., 2010; Smith & Blake, 2014). The geospatial characteristics (land use, catchment zone and erosion process) of each sample were identified on the PCA plot, facilitating a visual analysis of variance between potential geospatially relevant source groups. Additionally, the tracer vectors were plotted on the PCA ordination plot to check which tracers were responsible for the observed differences between the land-use types, catchment zones and erosion processes. The unsupervised clusters were subsequently plotted on the PCA plot and where necessary they were adapted to fit geospatially relevant groups. The PCA thus facilitated the comparison of the outcomes from the unsupervised CA with expert-based geospatial information, wherein source groups were created that are both statically and geospatially relevant (Pulley et al., 2017). Outlier samples were identified based on the distance from the centre of their most relevant cluster on the PCA plot. Gully samples were excluded from the $\delta^{13}\text{C}$ -FA fingerprint analysis because their low FA concentrations yielded unreliable $\delta^{13}\text{C}$ -FA measurements. The geochemical and $\delta^{13}\text{C}$ -FA fingerprints were analysed separately because of the high number of tracers with potentially overpowering signals that restricted detailed source grouping, and the unreliable subsurface $\delta^{13}\text{C}$ -FA fingerprints. Separate analysis of the biochemical and geochemical tracer sets thus allowed a more detailed and reliable source grouping, wherein nuanced differences in fingerprint between respective land-use types and erosion processes could be detected. The ordination plot of the composite fingerprint can be found in Figure S2.

2.4.2 | Bayesian mixing model

The source classes can be represented as multivariate concentration matrices upon which the model draws to proportionally attribute different sources to the riverine or deposited sediment. A BMM was created for this purpose within the MixSIAR framework (Stock et al., 2018; Stock & Semmens, 2016), which is implemented as an open-source R package (Stock & Semmens, 2017) and adapted by Blake et al. (2018a) for river basin sediment transport. The covariance structure of MixSIAR handles redundancy so tracer selection by discriminant function analysis is not required (Stock et al., 2018). As demonstrated by Smith et al. (2018), the most accurate source apportionment results in BMMs are achieved by a tracer selection procedure that only removed tracers on the basis of non-conservative behaviour. Each tracer was evaluated separately in each of the three river systems in the context of the specific environment and their environmental behaviour. Conservative behaviour of the tracers (Belmont et al., 2014; Koiter et al., 2013; Lizaga et al., 2020b) was tested using the simple tracer screening approach of Blake et al. (2018a) and Sherriff et al. (2015), wherein the tracer concentration range between sources and mixture was tested (Figures S3–S6). If the mean tracer concentration of the mixture was found to be outside the mean concentrations of the different sources, the tracer was excluded out of the analysis. These observations can be linked to non-conservative behaviour through enrichment or depletion processes (Wynants et al., 2020), but can also be due to pollution or sampling constraints in the case that certain tracers occur spatially concentrated in the catchment (Belmont et al., 2014; Yu & Oldfield, 1993). Furthermore, if the range test demonstrated the intra-source variance to be higher than the inter-source variance for specific tracers or if the inter-mixture variance was too high, they were also removed. Finally, the univariate tracer distributions of the riverine sediment were assessed for normality using the 'Shapiro–Wilk test' because the model assumes that mixture tracer data are normally distributed. If the tracer mixtures were not normally distributed, they were also removed from the analysis.

Based on these multiple tests, 12 tracers were excluded in the Ar dai system (Al_2O_3 , Ce, Cl, Ga, La, Mn, Na_2O , Ni, Pb, Th, Y and Zr), 12 in the Nanja (Al_2O_3 , Br, Ce, Cl, Ga, La, Mg, Nb, Nd, Pb, Sr and Zr), and 12 in the Musa (Ce, Cl, Co, Cu, Ga, K_2O , La, Na_2O , Nd, Pb, Th and Zn). Moreover, in the Ar dai, $\delta^{13}\text{C}$ -FA C25, C27, C29 and C31 were removed because they had a low abundance resulting into higher uncertainties and missing values. The ultimate tracer selection for the riverine BMM is given in Table 2.

Further model specifications included: a 'residual error' formulation, an uninformative prior, and no fixed effects. For all MixSIAR model runs, the Markov Chain Monte Carlo (MCMC) parameters were generally set as follows: chain length = 3,000,000, burn = 2,700,000, thin = 500, chains = 3. Convergence of model chain output was evaluated using the Gelman–Rubin diagnostics (Gelman et al., 2013), rejecting model output if any of the variables was above 1.05 confidence interval, in which case the chain length was increased. Non-convergence at high chain lengths indicates that the model cannot find a solution to the given set of sources and mixture, and can be caused by large intra-source variance, source fingerprint overlap, or a large mixture fingerprint. (Stock et al., 2018). If this was the case, the source grouping, explained in the previous section, was re-evaluated.

TABLE 2 An overview of selected tracers for soil-to-sediment Bayesian mixing model (BMM) based on the tracer screening approach

Ardai	Nanja	Musa
δ^{13} (C22, C23, C24, C26, C28, C30, C32), Ba, CaO, Co, Cu, Fe ₂ O ₃ , K ₂ O, MgO, Nb, P ₂ O ₅ , Rb, SiO ₂ , SO ₃ , Sr, Ti, Zn	Ba, CaO, Co, Cr, Cu, F, Fe ₂ O ₃ , K ₂ O, Mn, Na ₂ O, Ni, P ₂ O ₅ , Rb, SiO ₂ , SO ₃ , Th, Ti, Y, Zn	Al ₂ O ₃ , Ba, Br, CaO, Cr, Fe ₂ O ₃ , MgO, Mn, Nb, Ni, P ₂ O ₅ , Rb, SiO ₂ , SO ₃ , Sr, Ti, Y, Zr

Model outcomes are probability plots, wherein the mean of the plots is given as the proportional contribution of the sources and the standard deviation (SD) as an indicator of variability.

3 | RESULTS

3.1 | Source fingerprint analysis and -grouping

3.1.1 | Ardai

PCA of the geochemical Ardai soil samples (Figure 2A) revealed a complex soil system with variability on two levels of interest. The strongest distinction was found between the different catchment zones: low-zone, mid-zone and up-zone, signalling altitude-related differences in lithology, land cover and pedogenesis. The low-zone soils are characterized by higher concentrations of K₂O, Na₂O and MgO. Furthermore, they have a partly overlapping signal with SiO₂ and Rb.

The wetter up-zone soils have a distinct signal of P₂O₅ and SO₃ and are further characterized by high concentrations of CaO, Cl and Zn. These results already expose an important overlap between land use and catchment zones since certain land-use types are more or less constrained to certain catchment zones. Interestingly, the mid-zone samples formed two separate clusters. The first group of mid-zone soil samples took a central location on the PCA plot that probably indicates the intermediate between the up-zone and low-zone geochemical signals. The second mid-zone group is characterized by a clear signal from Ti, Fe₂O₃, Co, Nb, Al₂O₃ and Zr, and were grouped as a separate 'saprolite' class. Besides zonal grouping, the analysis also revealed a soil depth signal (surface vs. subsurface). About half of gully samples were characterized by SiO₂, Rb and Na₂O. Interestingly, the other gully samples clearly fell within one of the two mid-zone clusters and were therefore classified within those mid-zone clusters.

Exploration of the Ardai δ^{13} C-FA PCA plot (Figure 3A) reveals that soils in the up-zone have lower δ^{13} C signatures compared to the low zone. The most distinct cluster consists out of 'up-zone forest' samples, which is mostly characterized by low δ^{13} C-FA (C3 dominated vegetation). Interestingly, another distinct cluster consist mainly of the 'up-zone agriculture' and is characterized by slightly higher δ^{13} C-FA values (especially for the heavier C28–C32) compared to forest. Partly overlapping with both up-zone groups is a cluster of closed and open rangeland. The fourth and fifth cluster are characterized by 'maize cropland' and 'open rangeland' samples respectively. Substantial overlap between those groups is evident, however, is mostly due to one 'outlier' low-zone maize sample.

3.1.2 | Nanja

Geochemical analysis of the Nanja soil samples indicates clear clustering by catchment zone, and to a lesser extent, soil depth and land use (Figure 4A). One outlier gully sample (Arkaria gully 240–250 cm depth) was omitted from the analysis because it had unusually high concentrations of Ni, Cu, Zn and Cr, which might be due to a spatially isolated concentration of metals in the specific soil layer. Inclusion of this sample might skew the entire model away from gully contribution. A slight distinction was observed between the eastern (Arkaria) and western (Lepurko) rangelands. The 'western mid-zone open rangeland' soils overlapped with 'western closed bushland' soils and were therefore grouped into one class.

Furthermore, the 'mid-zone maize' samples clustered together nicely and were therefore kept in their own separate class. In the low zone, the surface 'maize cropland' and surface 'open rangeland' soil samples showed substantial overlap and were therefore grouped into one 'low-zone surface' class. The 'low-zone surface' samples were characterized by Na₂O, K₂O, SiO₂ and Rb. One shallow gully sample (< 30 cm) from the low-zone was integrated within this cluster. The gully samples demonstrated a high geochemical variability, but could be grouped into three major classes. Bed gullies were also characterized by SiO₂ and Rb, but not by Na₂O and K₂O. The other two gully classes were characterized by high concentrations of transition metals (Ni, Cu, Zn and Cr), with two distinct intensities that seem to be related to the catchment location (east vs. west).

3.1.3 | Musa

Analysis of the Musa soil samples shows distinct clustering that is mainly driven by geochemical differences between catchment zones on the one hand and soil depth on the other hand (Figure 5A). The up-zone surface soils are characterized by high concentrations of P₂O₅ and SO₃, as well as high concentrations of Br and CaO. The forest fingerprint slightly diverges from the up-zone agricultural fingerprint and can be grouped into two distinct sub-clusters (with four and two samples, respectively), wherein the latter seem to be driven by a weathering signal. Furthermore, the forest soils have higher concentration of SO₃, while the agricultural soils have a higher concentration of SiO₂, which could be a site-specific indication of a higher sand content in the latter. The up-zone agricultural soils form a distinct cluster with smaller sub-clusters between the different agricultural practices that slightly overlap.

The mid-zone surface soils also group into one distinct cluster with two sub-clusters of rangeland and maize cropland, and are mainly characterized by MgO, Sr, SiO₂ and Ba. At the same time, the mid-zone (older) soils have higher concentrations of transition metals (Zr, Nb and Mn) compared to the up-zone (younger) soils, but lower compared to the gullies. The up-zone and mid-zone gullies group into separate distinct clusters. The up-zone gullies are characterized by a distinct weathering signal: Fe₂O₃, Ti, Y, Ni, Cr, Al₂O₃, while the mid-zone gullies by the transition metals: Zr, Nb and Mn. However, the mid-zone gullies also have relatively high concentrations of the weathering tracers, albeit lower than the up-zone gullies, and at the same time have a tracer signal from Rb. Based on the PCA cluster analysis, the Musa soil samples could be grouped into five source

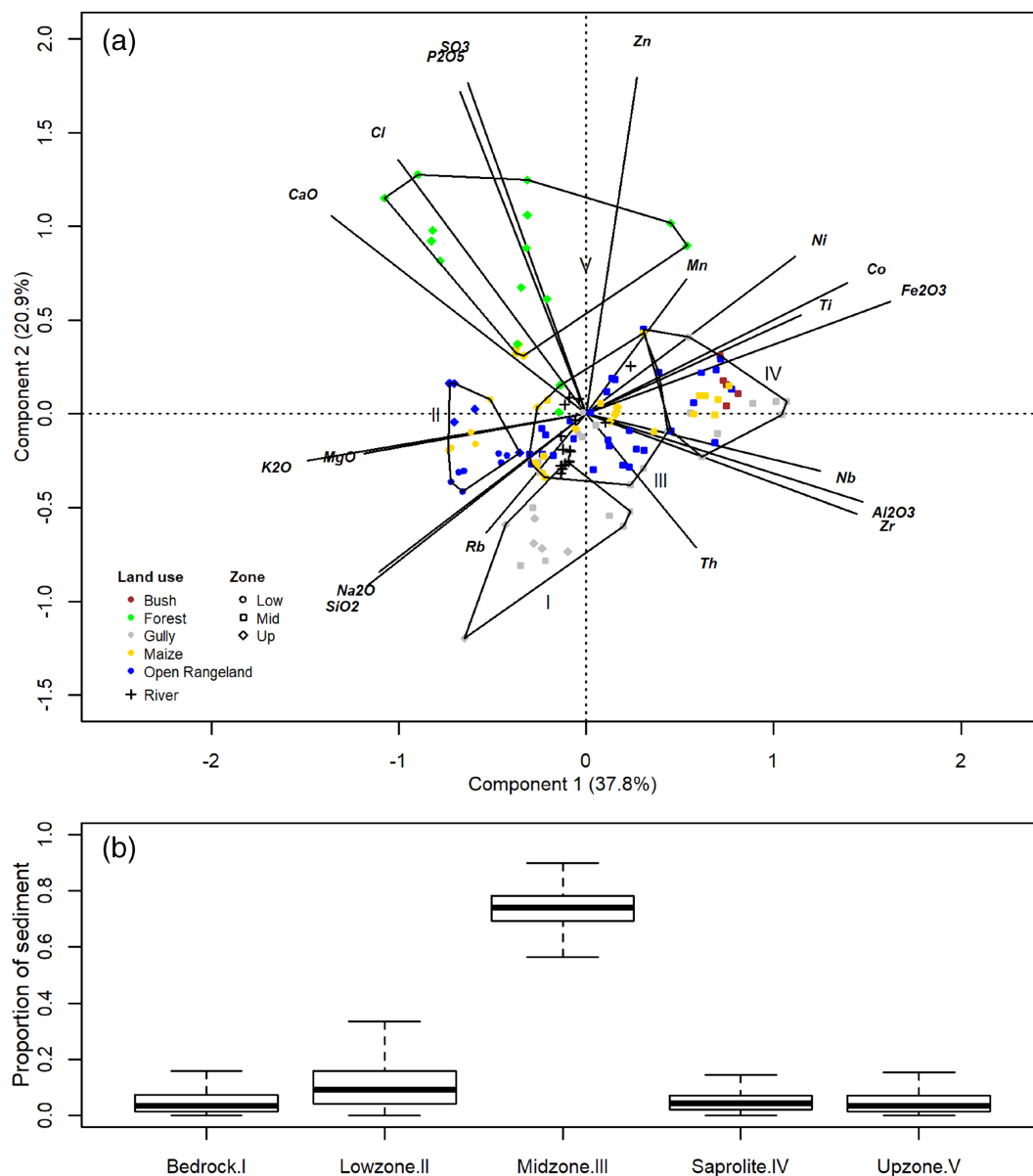


FIGURE 2 (A) PCA plot of soil and river geochemical fingerprint signals in the Ar dai sub-catchment with hull areas drawn around the soil groups as classified from the source grouping. Each group is given a number: I = bedrock incision, II = low-zone, III = mid-zone, IV = saprolites, V = up-zone. Each soil sample has been given a unique colour and symbol depending on respectively the land use and catchment zone where it was sampled from. (B) The output from the BMM that unimixed the sediment mixture against the soil groups in the Ar dai sub-catchment using their geochemical fingerprints. The boxplots represent the density distribution of the output from MCMC runs with median shown by central line, interquartile range by box, and range by whiskers. The boxplots thus indicate the contributions of each of the soil groups to the riverine sediment. The bigger the box and whiskers, the higher the probability range, meaning less certainty of the results. The numbers of the boxplot groups correspond with the numbers of the soil groups on the PCA plot [Color figure can be viewed at wileyonlinelibrary.com]

classes: ‘up-zone forest’, ‘up-zone mixed agriculture’, ‘mid-zone surface’ (rangeland + maize), ‘up-zone gullies’, and ‘mid-zone gullies’.

3.2 | Bayesian source apportionment

The geochemical BMM output from the Ar dai data (Figures 2B and S7A) is very distinct and points towards the soils of the mid-zone as the major contributing source of the Ar dai riverine sediment with 72.5% (SD = ±9.6%). Other sources are small but still significant, with low-zone soils contributing 11.1% (SD = ±8.7%), up-zone soils 5.5% (SD = ±7.5%), and the saprolite 5% (SD = ±3.6%). Finally, 6% (SD = ±9.0%) of sediment is attributed to bedrock incision processes.

It should be noted that the contributions from the mid-zone and saprolite group are both from hillslope sheet and incision processes. Output from the $\delta^{13}\text{C}$ -FA BMM (Figures 3B and S7B) points toward two major land-use sources of sediment: ‘open rangeland’ with 63.6% (SD = ±9.3%) and ‘maize cropland’ with 24.7% (SD = ±12.4%). ‘Upland agriculture’ contributes 4.8% (SD = ±3.7%) of the sediment, while ‘bushland’ and ‘upland forest’ respectively contribute 4.3% (SD = ±3.8%) and 2.4% (SD = ±2.1%) to the Ar dai riverine sediment. Integration of the geochemical and biochemical evidence bases was possible because the land-use types are more or less constrained to specific catchment zones. The land-use contributions were rescaled per catchment zone and subsequently multiplied with the specific zonal contributions to yield the zonal land-use groups. Low-zone

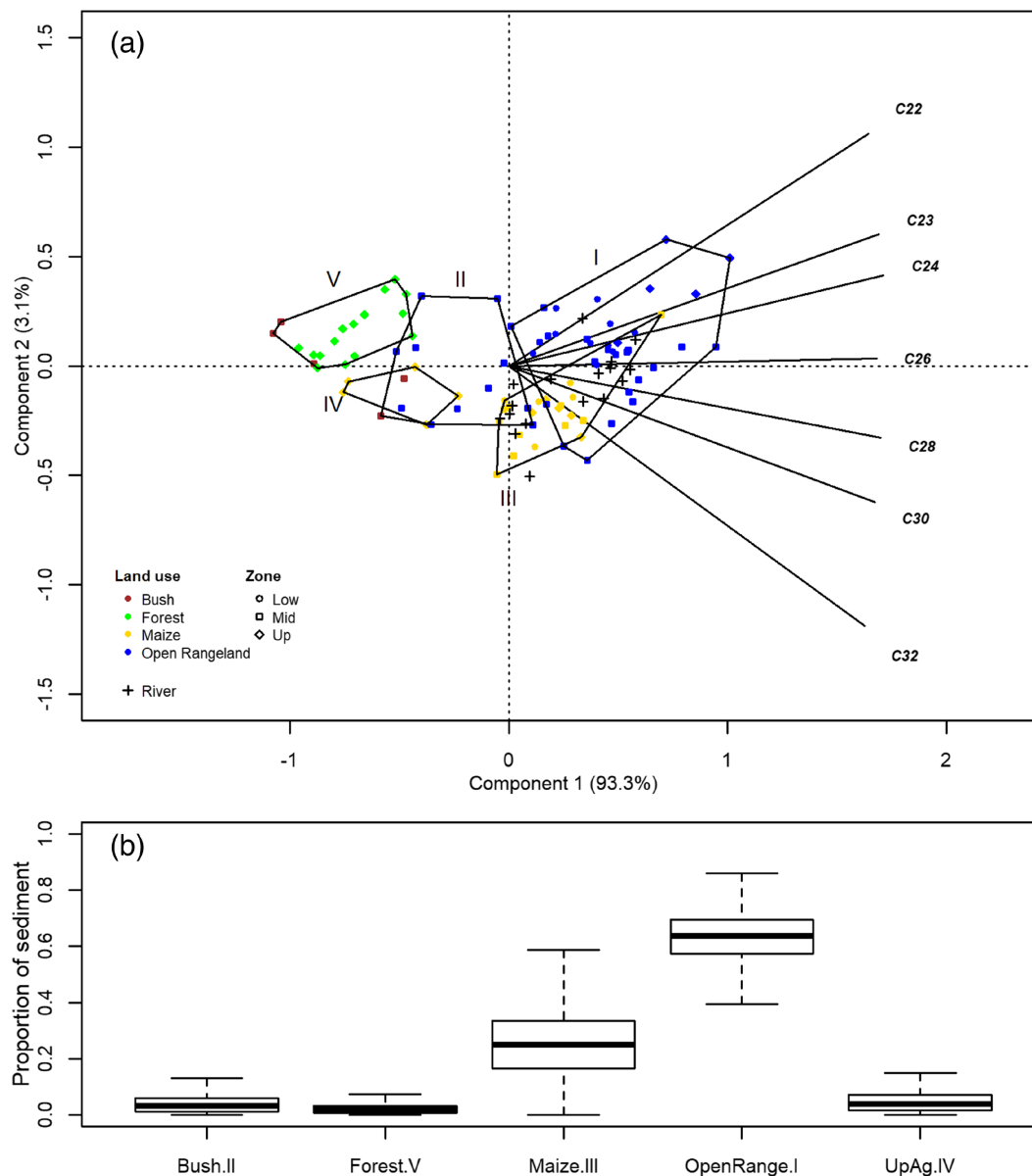


FIGURE 3 (A) PCA plot of soil and river biochemical tracer ($\delta^{13}\text{C}$ -FA) fingerprint signals in the Ar dai sub-catchment with hull areas drawn around the soil groups as classified from the source grouping. Each group is given a number: I = open rangeland, II = bushland, III = maize, IV = up-zone agriculture, V = forest. Each soil sample has been given a unique colour and symbol depending on respectively the land use and catchment zone where it was sampled from. (B) The output from the BMM that unmixed the sediment mixture against the soil groups in the Ar dai sub-catchment using their $\delta^{13}\text{C}$ -FA fingerprints. The boxplots represent the density distribution of the output from MCMC runs with median shown by central line, interquartile range by box, and range by whiskers. The boxplots thus indicate the contributions of each of the soil groups to the riverine sediment. The bigger the box and whiskers, the higher the probability range, meaning less certainty of the results. The numbers of the boxplot groups correspond with the numbers of the soil groups on the PCA plot [Color figure can be viewed at wileyonlinelibrary.com]

results were integrated with maize and open rangeland. Up-zone results were integrated with the upland agriculture and forest outcomes. Mid-zone and saprolite hillslopes were combined and integrated with maize, open range and closed range. Bedrock incision was kept separate, as it is independent from land use and catchment zone. The outcome of the integration (Figure 6) illustrates that hillslope erosion on the 'mid-zone rangelands' and 'mid-zone maize croplands' are the major sediment sources (52.4% and 21.4%, respectively) to the Ar dai River.

The geochemical BMM output from the Nanja sub-catchment (Figures 4B and S7C) points to the rangelands in the eastern mid-zone as the major source of sediment of the downstream Nanja River with 82.6% (SD = $\pm 5.2\%$). Other sources were found to be minimal, but

not insignificant. Bedrock, eastern and western hillslope gullies were found to contribute 2.5% (SD = $\pm 2.5\%$), 2.0% (SD = $\pm 1.5\%$) and 2.5% (SD = $\pm 2.8\%$) of the eroded sediment respectively. Low-zone surface erosion was attributed 4.2% (SD = $\pm 3.8\%$) of the sediment, mid-zone maize 2.7% (SD = $\pm 2.5\%$), and the western mid-zone rangelands 3.4% (SD = $\pm 3.2\%$).

The geochemical BMM of the Musa riverine sediment produced highly distinct source attributions of the source-classes (Figures 5B and S7D). 79.8% (SD = $\pm 3.6\%$) of the riverine sediment was attributed to sheet erosion from the 'mid-zone maize and rangelands'. The second major source to the riverine sediment was found to be 'mixed upland agriculture' with 15.8% (SD = $\pm 3.7\%$). The contributions of 'up-zone forest' (mean = 1.6%, SD = $\pm 1.7\%$), 'up-zone gullies'

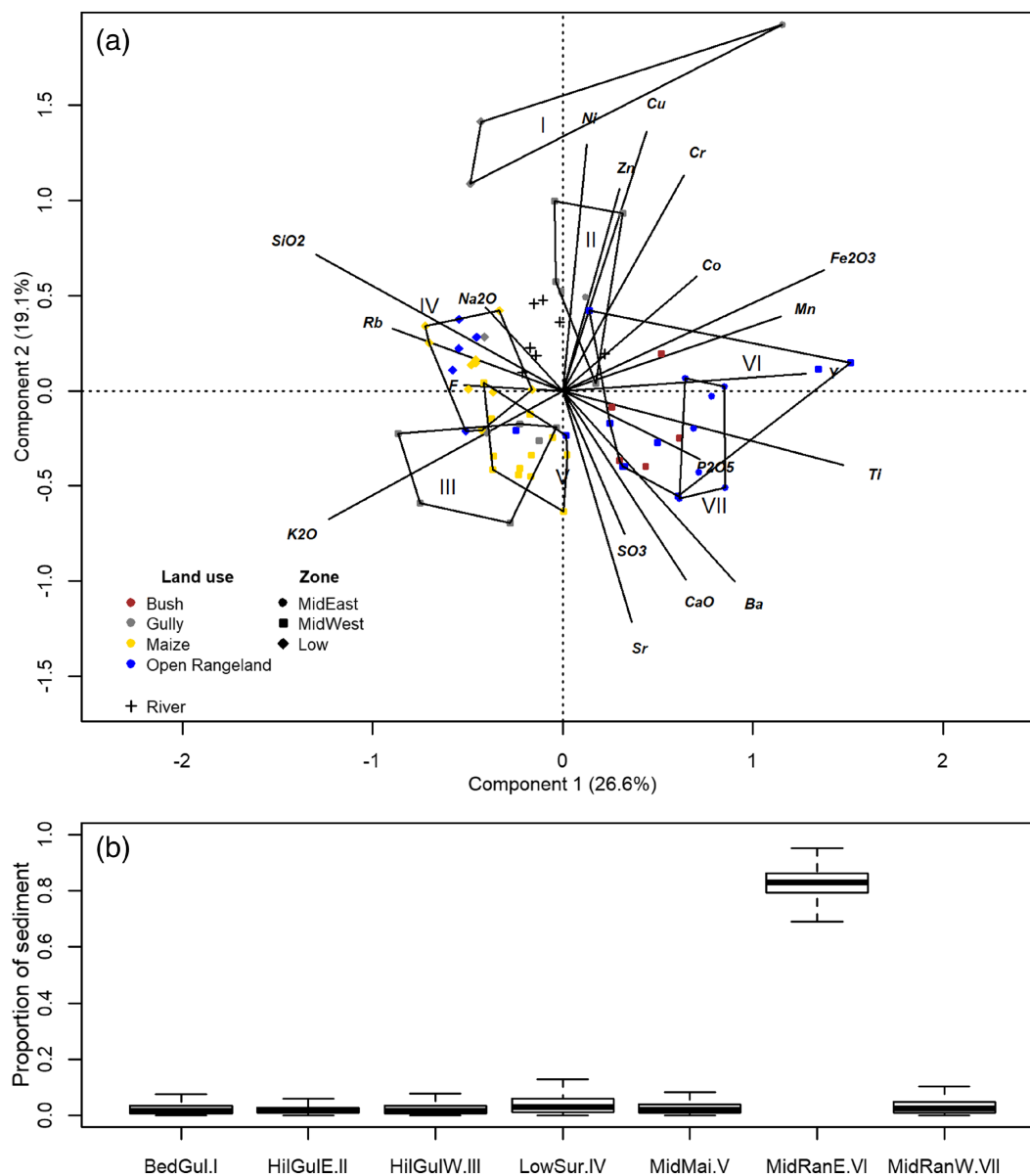


FIGURE 4 (A) PCA plot of soil and river geochemical fingerprint signals in the Nanja sub-catchment with hull areas drawn around the soil groups as classified from the source grouping. Each group is given a number: I = bedrock incision, II = eastern hillslope gullies, III = western hillslope gullies, IV = low-zone surface, V = mid-zone maize, VI = eastern mid-zone rangelands, VII = western mid-zone rangelands. Each soil sample has been given a unique colour and symbol depending on respectively the land use and catchment zone where it was sampled from. (B) The output from the BMM that unmixes the sediment mixture against the soil groups in the Nanja sub-catchment using their geochemical fingerprints. The boxplots represent the density distribution of the output from MCMC runs with median shown by central line, interquartile range by box, and range by whiskers. The boxplots thus indicate the contributions of each of the soil groups to the riverine sediment. The bigger the box and whiskers, the higher the probability range, meaning less certainty of the results. The numbers of the boxplot groups correspond with the numbers of the soil groups on the PCA plot [Color figure can be viewed at wileyonlinelibrary.com]

(mean = 1.4%, SD = $\pm 1.3\%$), and 'mid-zone gullies' (mean = 1.3%, SD = $\pm 1.4\%$) were minimal.

4 | DISCUSSION

4.1 | Source fingerprint analysis

The geochemical fingerprint analysis revealed a clear zonal signal in all three sub-catchments and a complex signal of gully incision, wherein gullies have highly variable signatures (Figures 2A, 4A and 5A). In all three catchments, the low-zone soils are characterized by an

evaporative signal (K_2O , Na_2O and MgO), which is due to their drier and hotter conditions that lead higher concentrations of salts on the soil surface, but also by higher SiO_2 concentrations that signal higher sand content (Horowitz, 1991). The wetter up-zone soils have a distinct detrital signal (P_2O_5 , SO_3 and CaO) due to the higher amounts of OM. This also indicates that land-use/vegetation patterns are not independent to catchment zones. While these zonal trends dominate the differences in geochemical fingerprints, the remaining importance of location-specific pedogenetic processes is evident from the distinct differences between surface soils of the same catchment altitude zone (Little & Lee, 2010). In the Nanja and Ar dai catchments, about half of the gullies and all river banks were characterized by less-

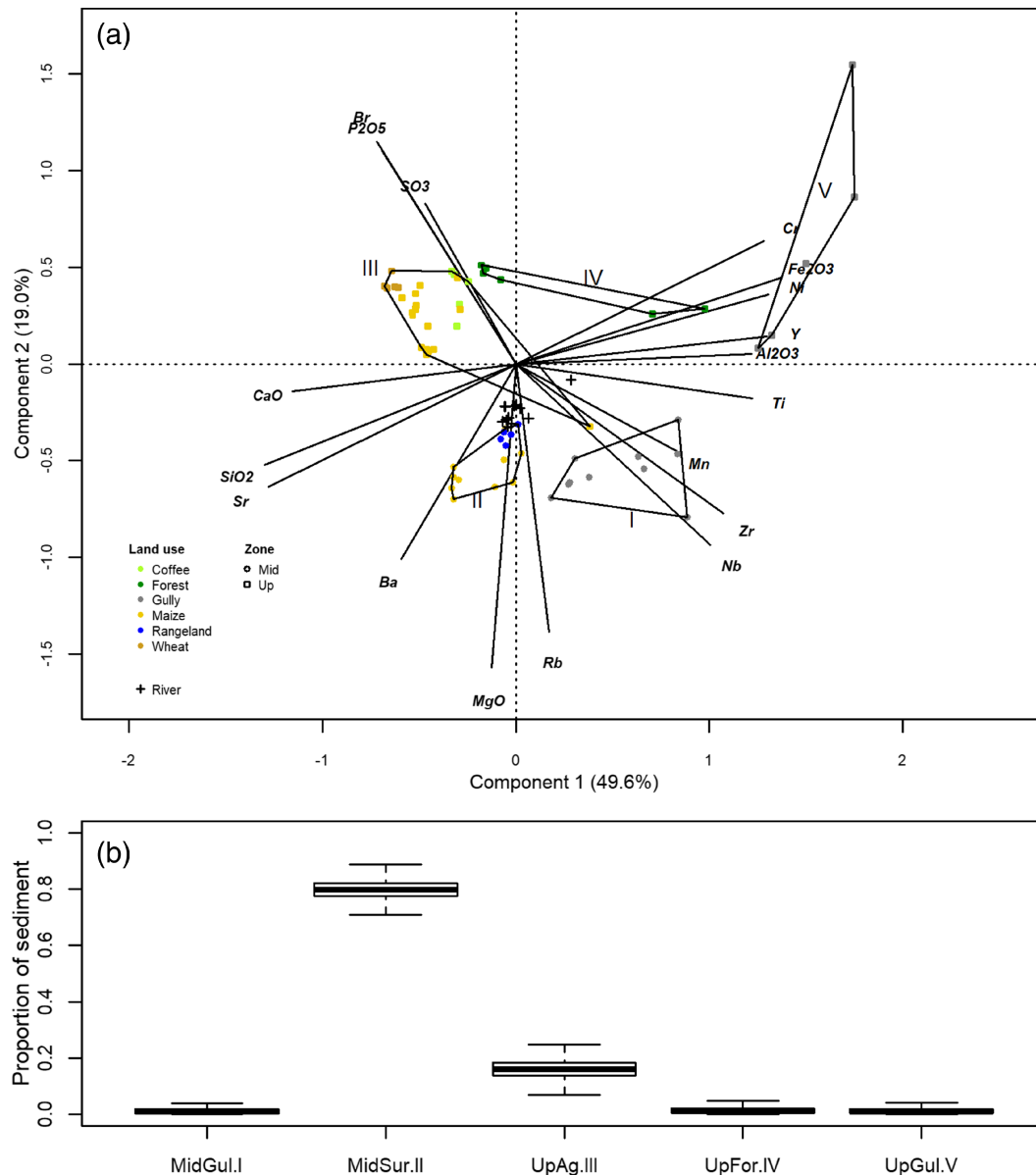


FIGURE 5 (A) PCA plot of soil and river geochemical fingerprint signals in the Musa sub-catchment with hull areas drawn around the soil groups as classified from the source grouping. Each group is given a number: I = mid-zone gullies, II = mid-zone surface, III = up-zone mixed agriculture, IV = up-zone forest, V = up-zone gullies. Each soil sample has been given a unique colour and symbol depending on respectively the land use and catchment zone where it was sampled from. (B) The output from the BMM that unmixed the sediment mixture against the soil groups in the Musa sub-catchment using their geochemical fingerprints. The boxplots represent the density distribution of the output from MCMC runs with median shown by central line, interquartile range by box, and range by whiskers. The boxplots thus indicate the contributions of each of the soil groups to the riverine sediment. The bigger the box and whiskers, the higher the probability range, meaning less certainty of the results. The boxplots indicate the contributions of each of the soil groups to the sediment. The numbers of the boxplot groups correspond with the numbers of the soil groups on the PCA plot [Color figure can be viewed at wileyonlinelibrary.com]

weathered tracers (SiO_2 , Rb), indicating they are incising closer to the bedrock (Baskaran, 2011; Horowitz, 1991). Interestingly, the other half had similar fingerprints as the surface soils. Moreover, some of the deep gullies were characterized by a strong weathering signal (Ti, Fe_2O_3 and Al_2O_3), which seems counterintuitive as deeper soil layers are usually less weathered as they are closer to the bedrock. However, soils in East Africa can be deeply weathered (Jones et al., 2013) and incision into these deep saporolites (Figure 7) can increase the strength of the weathering signal because they are not ‘diluted’ with detrital or evaporative surface signals. This observed lack of distinction complicates the eventual attribution of eroded sediment into surface and subsurface soils, which is a major limitation of erosion

process attribution in tropical areas. Moreover, while gullies can look similar, they can have originated from different hydrological processes.

Vice versa, the runoff processes that cause sheet erosion, are also responsible for hillslope gully incision. The distinction between surface and gully erosion is thus not clear-cut, and increased rates of sheet erosion can evolve into gully incision due to continued soil weakening and deepening rills (Figures 8 and 9). The ambivalence in gully fingerprints found in this study thus confirms existing knowledge about the complexity of gully erosion (Poesen, 2011; Valentin et al., 2005). Only in the Musa sub-catchment there was a clear distinction between the gully and surface fingerprints, wherein the former had a distinct

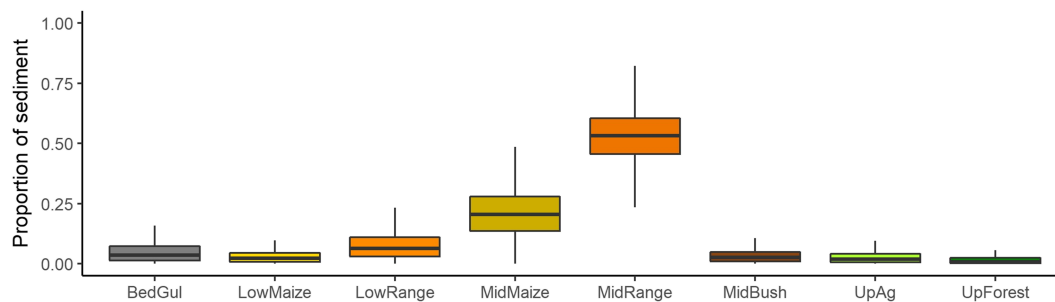


FIGURE 6 Boxplot of integrated geochemical and biochemical ($\delta^{13}\text{C}\text{-FA}$) results from the Ar dai catchment, showing the estimated contributions of bedrock incision (BedGul), low-zone maize croplands (LowMaize), low-zone open rangelands (LowRange), mid-zone maize croplands (MidMaize), mid-zone open rangelands (MidRange), mid-zone bushlands (MidBush), up-zone mixed agriculture (UpAg), and up-zone forest (UpForest). The boxplots represent the density distribution of the integrated results with median shown by central line, interquartile range by box, and range by whiskers [Color figure can be viewed at [wileyonlinelibrary.com](#)]



FIGURE 7 Gully incision on deeply weathered saprolites in the mid-zone hillslopes (latitude: -3.334067° , longitude: 36.360801°). The gully was > 7 m deep at some places and did not hit the bedrock [Color figure can be viewed at [wileyonlinelibrary.com](#)]



FIGURE 8 Exposed plant root evidence of > 2 cm topsoil removal on rangelands by sheet erosion (latitude: -3.333751° , longitude: 36.360225°), and evidence of surface crusting and rill erosion (latitude: -3.410499° , longitude: 36.407072°) in the mid- and low-zone rangelands [Color figure can be viewed at [wileyonlinelibrary.com](#)]

weathering signal which you would normally expect from surface soils. However, only three different locations with gully systems were sampled in Musa and the geochemical variability of gullies found in the other catchments might simply not have been captured in Musa. Similar to the other two sub-catchments, the ‘sheet erosion’ section in the Musa sub-catchment is thus likely to include hillslope incision processes as well. This exposes an important limitation in the methodology related to the limited spatial extent of soil and gully samples in the sub-catchments (Haddadchi et al., 2019; Yu & Oldfield, 1993).

The $\delta^{13}\text{C}\text{-FA}$ analysis of the Ar dai soils accentuates that in East African Rift systems, the $\delta^{13}\text{C}\text{-FA}$ fingerprint is mainly driven by the

altitude-rainfall gradient, working through the C3/C4 metabolic and altitude effects on the plant $\delta^{13}\text{C}$ signal (Upadhayay et al., 2020). In general, woody C3 plants with lower $\delta^{13}\text{C}$ dominate the wetter up-zone, while grass C4 plants with higher $\delta^{13}\text{C}$ values dominate the drier low-zone (Osborne, 2008). As maize is a C4 plant, soils under the dominant maize cropping systems will also incorporate a C4 signal (Christensen et al., 2011). Besides the altitudinal C3–C4 gradient, $\delta^{13}\text{C}\text{-FA}$ is additionally influenced by altitude through the effects of vapour pressure deficit, temperature, and CO_2 concentration on plant photosynthetic activity and stomatal conductance (Upadhayay et al., 2020). Nonetheless, as dominant land-use types also often correspond with catchment zones, CSIA is still a robust tool for land-use

FIGURE 9 Interlinking of sheet erosion with lateral and upslope progression of gullies leading to badland formation in the mid-zone. Exposed roots indicate over 50 cm of soil removal (latitude: -3.316011° , longitude: 36.423080°) [Color figure can be viewed at wileyonlinelibrary.com]



FIGURE 10 Soil conservation practices on the up-zone agricultural lands with contour terraces that are buffered by permanent vegetation strips (latitude: -3.301534° , longitude: 36.519732°) [Color figure can be viewed at wileyonlinelibrary.com]



attribution to the sediment. This is confirmed in our results, where the most distinct cluster consists out of C3 dominated up-zone forest, characterized by low $\delta^{13}\text{C}$ -FA. Up-zone agriculture also formed a distinct group, which could be due to the mixture of the dominant maize crop with a residual forest signal, crop rotations with C3 types, the general wetter conditions allowing C3 weed growth, the presence of trees on the terrace boundaries (Figure 10), and/or the altitude effects on maize $\delta^{13}\text{C}$ -FA signal.

Partly overlapping with both up-zone groups was a cluster of closed and open rangeland, which probably signals a transition zone from woody to grass vegetation. Moreover, the biochemical fingerprint of 'open rangelands' and 'maize croplands' in the same catchment zone still diverged slightly, highlighting the power of using compound specific FA fingerprinting compared to bulk $\delta^{13}\text{C}$ or $\delta^{15}\text{N}$. While substantial overlap was still evident between these two

groups, this was mostly due to one outlier. Moreover, as shown by Wynants et al. (2018), rangelands are the major source of new maize cropping land. Vice versa, maize crops are often abandoned and return to rangeland. These changes in land cover leave a residual signal in the soil (Blake et al., 2012). Furthermore, the maize growing season is short and even during the growing season it is highly likely that the plots are re-colonized by natural grassland plants (Nassary et al., 2020).

4.2 | Sources of eroded sediment

In the three river systems, the sediment is dominated by mid-zone 'open rangelands' and mid-zone 'maize croplands' sources. This finding corroborates with the results from Wynants et al. (2018), wherein

the mid-zone in the northern Makuyuni is highlighted as the area with the highest increase in erosion risk after land-cover change. Moreover, the observed dominance of 'maize cropland' and 'open rangeland' matches visual evidence of soil degradation and hillslope incision in the study area (Figures 8, 7, and 9) and measurements of low aggregate stability (Figure S8). The high contribution of 'open rangelands' can be explained by multiple environmental and anthropogenic factors. First, the 'open rangelands' constitute the largest area in the Ar dai catchment (Table 1) and can therefore potentially generate high quantities of sediment. Second, the 'open rangelands' have a seasonal vegetation cycle, partly exposing the soil in the dry season and making them naturally vulnerable for erosion at the start of the rainy season (Kirkby, 1980). Third, overgrazing in the region prohibits natural vegetation recovery, leading to a higher vulnerability to soil erosion and runoff generation (Hein, 2006). Finally, the high contribution of 'open rangelands' could also be partly explained by their clearance for conversion into 'maize croplands', wherein land clearance increases erosion and thereby also the contribution of soil from the cleared land use to the sediment (Lal, 1996). The high contribution of 'maize croplands' is also not surprising given its high vulnerability to soil erosion. The mid-zone and low-zone 'maize croplands' in the Makuyuni catchment are solely dependent on rainfall and are cleared for planting at the start of the rainy season (Trærup & Mertz, 2011). Furthermore, they only provide cover for a short period in the year and their superficial root system and row planting does not provide a solid buffer from erosion (Ngwira et al., 2013). Bedrock incision seems to only have a minor contribution to the total eroded sediment.

These findings in mid-sized catchments from Tanzania match those from agricultural headwater catchments in the highlands of southern Kenya, wherein agricultural surface soils were found to be the main source of riverine sediment (Kroese et al., 2020). However, it is important to note that the sediment samples were not taken continuously, and our results thus only represent the situation of the sampled time-period. Since river catchments systems are dynamic, they have variable amounts of discharge, sediment transport and source contributions (Lizaga et al., 2019, 2020a). This is especially so in the context of semi-arid East Africa, which is further explored in the paired article of Wynants et al. (2021). The lack of high temporal resolution sampling is thus a major source of uncertainty in this study. The multivariate fingerprint analysis did reveal that the variance between river sediment sampled from different time-periods and modes of sampling was relatively small compared to the variance between the potential sources, adding some robustness to the model outputs. Nonetheless, future sediment source tracing studies in East Africa will need to find innovative ways to obtain high temporal resolution sediment data from these highly unpredictable ephemeral systems. Moreover, as highlighted before, surface erosion and hillslope gully incision are not independent processes and were often found to resemble each other geochemically. The dominance of the hillslope source groups and low contribution from the bedrock incision source group should therefore not be interpreted as a lack of contribution from subsurface sources. Furthermore, in the context of catchment sediment connectivity, gullies also have an important effect on downstream sediment routing. While gully formation is usually mediated by farmers on private farms, limiting the downstream transport of eroded sediment, gullies often remain uncontrolled on the rangelands (Figures 7 and 9), speeding up hillslope degradation and downstream

connectivity (Blake et al., 2018b). The higher contribution of sediment from the 'open rangelands' is thus not only caused by higher rates of erosion, but by a higher connectivity with the river system. Furthermore, the rangelands are often situated in the mid-zone of the catchment with significant runoff contribution from upstream agricultural lands. A study by Blake et al. (2020) has shown that increased runoff from upstream agricultural areas can lead to increased erosion and gully incision on the downstream rangelands. The observed lower contribution of 'upland agriculture' can be explained by longer growing seasons, a more diverse crop selection with better soil cover, higher soil OM content and aggregate stability (Figure S8), and the presence of terraces and permanent vegetated buffer strips (Figure 10). Finally, the low contributions of 'bushland' and 'upland forest' shows that natural vegetation remains the best buffer for soil erosion and sediment transport, especially since these land-use types are currently constrained to the steepest areas in the catchment.

5 | CONCLUSION

Analysis of the potential source materials in the Ar dai, Nanja and Musa sub-catchments revealed a highly complex and variable earth surface system. Geochemical fingerprinting was shown to be a robust tool for distinguishing catchment zones. Biochemical $\delta^{13}\text{C}$ -FA fingerprinting was also dominated by the catchment zone, however, specific $\delta^{13}\text{C}$ for the different FA still made it possible to pick up nuanced differences between land-use types. Attribution of eroded sediment to subsurface erosion was complicated due to the variability in the geochemical subsurface source fingerprints. Nonetheless, sediment source tracing highlighted a dominance of hillslope erosion (both sheet erosion and gully incision on deep soils) from the mid-zone, contributing over 75% of the transported sediment in the three studied catchments. The main contributing land-use types are the 'open rangelands' and 'maize croplands'. Even though the mid-zone is the dominant source area of sediment, the current situation constitutes a highly connected landscape, where high amounts of eroded soils from all over the catchment are rapidly transported downstream.

By applying sediment source tracing, this study not only highlighted the dominant sources of eroded sediment in the specific catchments, but also elucidated some of the complex spatial dynamics of soil erosion and sediment transport in Tanzanian river systems. Urgent mitigative strategies for both the rangelands and croplands are required to stop the further acceleration of soil erosion and sediment transport, wherein both the soil erodibility and the landscape connectivity needs to be reduced. Future sediment source tracing studies in East Africa should not only aim to quantify the contribution of hillslope gullies to the total sediment load, but also obtain a better understanding of the role of gully incision as a positive feedback loop in the processes of hillslope degradation and sediment connectivity. In this context, the study also highlighted the need for novel tracers that can better distinguish between the surface and subsurface deeply weathered soils.

ACKNOWLEDGEMENTS

This work was carried out as part of a PhD project funded by University of Plymouth, Faculty of Science and Engineering, PhD Scholarship with additional support from European Commission (Horizon 2020

IMIXSED project ID 644320), the Research Council UK Global Challenges Research Fund (GCRF) grant NE/P015603/1 and UK Natural Environment Research Council Grant NE/R009309/1. The authors would also like to extend their gratitude to the wider research community at the Nelson Mandela Institution for Science and Technology in Arusha, Tanzania for their guidance and logistical support during the field campaigns. Moreover, the authors are indebted to Richard Hartley of the University of Plymouth for his technical support during the field and laboratory work. Finally, the authors are thankful to the reviewers for the thorough revisions that have significantly increased the quality of the output.

CONFLICT OF INTEREST

The authors have no conflict of interest to declare.

DATA AVAILABILITY STATEMENT

The raw dataset, model inputs, model build and model outputs are available open access on <https://doi.org/10.24382/9xmf-7e88>.

ORCID

Maarten Wynants  <https://orcid.org/0000-0002-5367-7619>

REFERENCES

- Alewel, C., Birkholz, A., Meusburger, K., Schindler Wildhaber, Y. & Mabit, L. (2016) Quantitative sediment source attribution with compound-specific isotope analysis in a C3 plant-dominated catchment (central Switzerland). *Biogeosciences*, 13(5), 1587–1596. <https://doi.org/10.5194/bg-13-1587-2016>
- Amasi, A., Wynants, M., Blake, W. & Mtei, K. (2021) Drivers, impacts and mitigation of increased sedimentation in the hydropower reservoirs of East Africa. *Land*, 10(6), 638. <https://doi.org/10.3390/land10060638>
- Baskaran, M. (2011) *Handbook of environmental isotope geochemistry*. Berlin: Springer Science & Business Media.
- Belmont, P., Willenbring, J.K., Schottler, S.P., Marquard, J., Kumarasamy, K. & Hemmis, J.M. (2014) Toward generalizable sediment fingerprinting with tracers that are conservative and nonconservative over sediment routing timescales. *Journal of Soils and Sediments*, 14(8), 1479–1492. <https://doi.org/10.1007/s11368-014-0913-5>
- Blake, W.H., Boeckx, P., Stock, B.C., Smith, H.G., Bodé, S., Upadhayay, H.R. et al. (2018a) A deconvolutional Bayesian mixing model approach for river basin sediment source apportionment. *Scientific Reports*, 8(1), 13073. <https://doi.org/10.1038/s41598-018-30905-9>
- Blake, W.H., Ficken, K.J., Taylor, P., Russell, M.A. & Walling, D.E. (2012) Tracing crop-specific sediment sources in agricultural catchments. *Geomorphology*, 139, 322–329.
- Blake, W.H., Kelly, C., Wynants, M., Patrick, A., Lewin, S., Lawson, J. et al. (2020) Integrating land-water-people connectivity concepts across disciplines for co-design of soil erosion solutions. *Land Degradation & Development*, 32(12), 3415–3430. <https://doi.org/10.1002/ldr.3791>
- Blake, W.H., Rabinovich, A., Wynants, M., Kelly, C., Nasser, M., Ngondya, I. et al. (2018b) Soil erosion in East Africa: An interdisciplinary approach to realising pastoral land management change. *Environmental Research Letters*, 13(12), 124014. <https://doi.org/10.1088/1748-9326/aaea8b>
- Borrelli, P., Robinson, D.A., Fleischer, L.R., Lugato, E., Ballabio, C., Alewell, C. et al. (2017) An assessment of the global impact of 21st century land use change on soil erosion. *Nature Communications*, 8(1), 2013. <https://doi.org/10.1038/s41467-017-02142-7>
- Borrelli, P., Robinson, D.A., Panagos, P., Lugato, E., Yang, J.E., Alewell, C. et al. (2020) Land use and climate change impacts on global soil erosion by water (2015–2070). *Proceedings of the National Academy of Sciences*, 117, 21994–22001.
- Christensen, B.T., Olesen, J.E., Hansen, E.M. & Thomsen, I.K. (2011) Annual variation in $\delta^{13}\text{C}$ values of maize and wheat: Effect on estimates of decadal scale soil carbon turnover. *Soil Biology and Biochemistry*, 43(9), 1961–1967. <https://doi.org/10.1016/j.soilbio.2011.06.008>
- Collins, A.L., Pulley, S., Foster, I.D.L., Gellis, A., Porto, P. & Horowitz, A.J. (2017) Sediment source fingerprinting as an aid to catchment management: A review of the current state of knowledge and a methodological decision-tree for end-users. *Journal of Environmental Management*, 194, 86–108. <https://doi.org/10.1016/j.jenvman.2016.09.075>
- Collins, A., Walling, D., Webb, L. & King, P. (2010) Apportioning catchment scale sediment sources using a modified composite fingerprinting technique incorporating property weightings and prior information. *Geoderma*, 155(3–4), 249–261. <https://doi.org/10.1016/j.geoderma.2009.12.008>
- Cooper, R.J., Krueger, T., Hiscock, K.M. & Rawlins, B.G. (2015) High-temporal resolution fluvial sediment source fingerprinting with uncertainty: A Bayesian approach. *Earth Surface Processes and Landforms*, 40(1), 78–92. <https://doi.org/10.1002/esp.3621>
- Dutton, C.L., Subalusky, A.L., Hill, T.D., Aleman, J.C., Rosi, E.J., Onyango, K.B. et al. (2019) A 2000-year sediment record reveals rapidly changing sedimentation and land use since the 1960s in the Upper Mara-Serengeti Ecosystem. *Science of the Total Environment*, 664, 148–160. <https://doi.org/10.1016/j.scitotenv.2019.01.421>
- FAO. (2019) *FAOSTAT statistical database*. Rome: Food and Agriculture Organization of the United Nations.
- Fenta, A.A., Tsunekawa, A., Haregeweyn, N., Poesen, J., Tsubo, M., Borrelli, P. et al. (2020) Land susceptibility to water and wind erosion risks in the East Africa region. *Science of the Total Environment*, 703, 135016. <https://doi.org/10.1016/j.scitotenv.2019.135016>
- Forgy, E.W. (1965) Cluster analysis of multivariate data: Efficiency versus interpretability of classifications. *Biometrics*, 21, 768–769.
- Fryirs, K. (2013) (Dis) Connectivity in catchment sediment cascades: A fresh look at the sediment delivery problem. *Earth Surface Processes and Landforms*, 38(1), 30–46. <https://doi.org/10.1002/esp.3242>
- Gellis, A.C. & Noe, G.B. (2013) Sediment source analysis in the Linganore Creek watershed, Maryland, USA, using the sediment fingerprinting approach: 2008 to 2010. *Journal of Soils and Sediments*, 13(10), 1735–1753. <https://doi.org/10.1007/s11368-013-0771-6>
- Gelman, A., Carlin, J.B., Stern, H.S., Dunson, D.B., Vehtari, A. & Rubin, D.B. (2013) *Bayesian data analysis*. London: Chapman and Hall/CRC 10.1201/b16018.
- Gibbs, M. (2008) Identifying source soils in contemporary estuarine sediments: A new compound-specific isotope method. *Estuaries and Coasts*, 31(2), 344–359. <https://doi.org/10.1007/s12237-007-9012-9>
- Guzha, A., Rufino, M., Okoth, S., Jacobs, S. & Nóbrega, R. (2018) Impacts of land use and land cover change on surface runoff, discharge and low flows: Evidence from East Africa. *Journal of Hydrology: Regional Studies*, 15, 49–67.
- Haddadchi, A., Hicks, M., Olley, J.M., Singh, S. & Srinivasan, M.S. (2019) Grid-based sediment tracing approach to determine sediment sources. *Land Degradation & Development*, 30(17), 2088–2106.
- Haddadchi, A., Ryder, D.S., Evrard, O. & Olley, J. (2013) Sediment fingerprinting in fluvial systems: review of tracers, sediment sources and mixing models. *International Journal of Sediment Research*, 28(4), 560–578. [https://doi.org/10.1016/S1001-6279\(14\)60013-5](https://doi.org/10.1016/S1001-6279(14)60013-5)
- Hardy, F., Bariteau, L., Lorrain, S., Theriault, I., Gagnon, G., Messier, D. & Rougerie, J.-F. (2010) Geochemical tracing and spatial evolution of the sediment bed load of the Romaine River, Quebec, Canada. *Catena*, 81(1), 66–76. <https://doi.org/10.1016/j.catena.2010.01.005>
- Hein, L. (2006) The impacts of grazing and rainfall variability on the dynamics of a Sahelian rangeland. *Journal of Arid Environments*, 64(3), 488–504. <https://doi.org/10.1016/j.jaridenv.2005.06.014>
- Heiri, O., Lotter, A.F. & Lemcke, G. (2001) Loss on ignition as a method for estimating organic and carbonate content in sediments: Reproducibility and comparability of results. *Journal of Paleolimnology*, 25(1), 101–110. <https://doi.org/10.1023/A:1008119611481>

- Hoffmann, T. (2015) Sediment residence time and connectivity in non-equilibrium and transient geomorphic systems. *Earth-Science Reviews*, 150, 609–627. <https://doi.org/10.1016/j.earscirev.2015.07.008>
- Horowitz, A.J. (1991) *A primer on sediment-trace element chemistry*. Vol. 2. Chelsea: Lewis Publishers.
- Jacobs, S.R., Timbe, E., Weeser, B., Rufino, M.C., Butterbach-Bahl, K. & Breuer, L. (2018) Assessment of hydrological pathways in East African montane catchments under different land use. *Hydrology and Earth System Sciences*, 22(9), 4981–5000. <https://doi.org/10.5194/hess-22-4981-2018>
- Janssens de Bisthoven, L., Vanhove, M.P.M., Rochette, A.J., Hugé, J., Verbesselt, S., Machunda, R. et al. (2020) Social-ecological assessment of Lake Manyara basin, Tanzania: A mixed method approach. *Journal of Environmental Management*, 267, 110594. <https://doi.org/10.1016/j.jenvman.2020.110594>
- Jones, A., Breuning-Madsen, H., Brossard, M., Dampha, A., Deckers, J., Dewitte, O. et al. (2013) *Soil atlas of Africa*. Luxembourg: Publications Office of the European Union European Commission.
- Kassambara, A. (2017) *Practical guide to cluster analysis in R: Unsupervised machine learning*. Sthda. sthda.com
- Kelly, C., Wynants, M., Munishi, L.K., Nasser, M., Patrick, A., Mtei, K.M. et al. (2020) ‘Mind the Gap’: Reconnecting local actions and multi-level policies to bridge the governance gap. An example of soil erosion action from East Africa. *Landscape*, 9, 352.
- Kirkby, M.J. (Ed.) (1980) *The problem*. In: *Soil erosion*. Chichester: Wiley.
- Kitch, J.L., Phillips, J., Peukert, S., Taylor, A. & Blake, W.H. (2019) Understanding the geomorphic consequences of enhanced overland flow in mixed agricultural systems: Sediment fingerprinting demonstrates the need for integrated upstream and downstream thinking. *Journal of Soils and Sediments*, 19(9), 3319–3331. <https://doi.org/10.1007/s11368-019-02378-4>
- Kiunsi, R. & Meadows, M. (2006) Assessing land degradation in the Monduli District, northern Tanzania. *Land Degradation & Development*, 17(5), 509–525. <https://doi.org/10.1002/ldr.733>
- Koiter, A., Owens, P., Petticrew, E. & Lobb, D. (2013) The behavioural characteristics of sediment properties and their implications for sediment fingerprinting as an approach for identifying sediment sources in river basins. *Earth-Science Reviews*, 125, 24–42. <https://doi.org/10.1016/j.earscirev.2013.05.009>
- Kroese, J.S., Batista, P.V., Jacobs, S.R., Breuer, L., Quinton, J.N. & Rufino, M.C. (2020) Agricultural land is the main source of stream sediments after conversion of an African montane forest. *Scientific Reports*, 10, 1–15.
- Lacey, J.P., Evrard, O., Smith, H.G., Blake, W.H., Olley, J.M., Minella, J.P. & Owens, P.N. (2017) The challenges and opportunities of addressing particle size effects in sediment source fingerprinting: A review. *Earth-Science Reviews*, 169, 85–103. <https://doi.org/10.1016/j.earscirev.2017.04.009>
- Lal, R. (1996) Deforestation and land-use effects on soil degradation and rehabilitation in western Nigeria. III. Runoff, soil erosion and nutrient loss. *Land Degradation & Development*, 7(2), 99–119. [https://doi.org/10.1002/\(SICI\)1099-145X\(199606\)7:2<99::AID-LDR220>3.0.CO;2-F](https://doi.org/10.1002/(SICI)1099-145X(199606)7:2<99::AID-LDR220>3.0.CO;2-F)
- Little, M. & Lee, C.-T. (2010) Sequential extraction of labile elements and chemical characterization of a basaltic soil from Mt. Meru, Tanzania. *Journal of African Earth Sciences*, 57(5), 444–454. <https://doi.org/10.1016/j.jafrearsci.2009.12.001>
- Lizaga, I., Gaspar, L., Blake, W.H., Latorre, B. & Navas, A. (2019) Fingerprinting changes of source apportionments from mixed land uses in stream sediments before and after an exceptional rainstorm event. *Geomorphology*, 341, 216–229. <https://doi.org/10.1016/j.geomorph.2019.05.015>
- Lizaga, I., Gaspar, L., Latorre, B. & Navas, A. (2020a) Variations in transport of suspended sediment and associated elements induced by rainfall and agricultural cycle in a Mediterranean agroforestry catchment. *Journal of Environmental Management*, 272, 111020. <https://doi.org/10.1016/j.jenvman.2020.111020>
- Lizaga, I., Latorre, B., Gaspar, L. & Navas, A. (2020b) Consensus ranking as a method to identify non-conservative and dissenting tracers in fingerprinting studies. *Science of the Total Environment*, 720, 137537. <https://doi.org/10.1016/j.scitotenv.2020.137537>
- Lowdermilk, W.C. (1953) *Conquest of the land through 7,000 years*. Washington, DC: US Department of Agriculture.
- Maerker, M., Quénéhervé, G., Bachofer, F. & Mori, S. (2015) A simple DEM assessment procedure for gully system analysis in the Lake Manyara area, northern Tanzania. *Natural Hazards*, 79(S1), 235–253. <https://doi.org/10.1007/s11069-015-1855-y>
- Maitima, J.M., Mugatha, S.M., Reid, R.S., Gachimbi, L.N., Majule, A., Lyaruu, H. et al. (2009) The linkages between land use change, land degradation and biodiversity across East Africa. *African Journal of Environmental Science and Technology*, 3(10), 310–325.
- Motha, J., Wallbrink, P., Hairsine, P. & Grayson, R. (2002) Tracer properties of eroded sediment and source material. *Hydrological Processes*, 16(10), 1983–2000. <https://doi.org/10.1002/hyp.397>
- Nachtergaele, F., Van Velthuizen, H., Verelst, L., Batjes, N., Dijkshoorn, J., Van Engelen, V., Fischer, G., Jones, A., Montanarella, L. & Petri, M. (2008) Harmonized World Soil Database (version 1.0). Food and Agriculture Organization of the United Nations (FAO); International Inst. for Applied Systems Analysis (IIASA); ISRIC-World Soil Information; Institute of Soil Science – Chinese Academy of Sciences (ISS-CAS); EC-Joint Research Centre (JRC).
- Nassary, E.K., Baijokya, F. & Ndakidemi, P.A. (2020) Intensification of common bean and maize production through rotations to improve food security for smallholder farmers. *Journal of Agriculture and Food Research*, 2, 100040. <https://doi.org/10.1016/j.jafr.2020.100040>
- Ngecu, W. & Mathu, E. (1999) The El-Nino-triggered landslides and their socioeconomic impact on Kenya. *Environmental Geology*, 38(4), 277–284. <https://doi.org/10.1007/s002540050425>
- Ngwira, A., Thierfelder, C., Eash, N. & Lambert, D.M. (2013) Risk and maize-based cropping systems for smallholder Malawi farmers using conservation agriculture technologies. *Experimental Agriculture*, 49(4), 483–503. <https://doi.org/10.1017/S0014479713000306>
- Nicholson, S.E. (1996) A review of climate dynamics and climate variability in Eastern Africa. In: Johnson, T.C. & Odada, E.O. (Eds.) *The limnology, climatology and paleoclimatology of the East African lakes*. Amsterdam: Gordon and Breach Publishers.
- Olago, D.O. & Odada, E.O. (2007) Sediment impacts in Africa’s trans-boundary lake/river basins: Case study of the East African Great Lakes. *Aquatic Ecosystem Health & Management*, 10(1), 23–32. <https://doi.org/10.1080/14634980701223727>
- Osborne, C.P. (2008) Atmosphere, ecology and evolution: What drove the Miocene expansion of C4 grasslands? *Journal of Ecology*, 96, 35–45.
- Owens, P., Blake, W., Gaspar, L., Gateuille, D., Koiter, A., Lobb, D. et al. (2016) Fingerprinting and tracing the sources of soils and sediments: Earth and ocean science, geoarchaeological, forensic, and human health applications. *Earth-Science Reviews*, 162, 1–23. <https://doi.org/10.1016/j.earscirev.2016.08.012>
- Poesen, J. (2011) Challenges in gully erosion research. *Landform Analysis*, 17, 5–9.
- Prins, H. & Loth, P. (1988) Rainfall patterns as background to plant phenology in northern Tanzania. *Journal of Biogeography*, 15(3), 451–463. <https://doi.org/10.2307/2845275>
- Pulley, S., Foster, I. & Collins, A.L. (2017) The impact of catchment source group classification on the accuracy of sediment fingerprinting outputs. *Journal of Environmental Management*, 194, 16–26. <https://doi.org/10.1016/j.jenvman.2016.04.048>
- Reiffarth, D., Petticrew, E., Owens, P. & Lobb, D. (2016) Sources of variability in fatty acid (FA) biomarkers in the application of compound-specific stable isotopes (CSSIs) to soil and sediment fingerprinting and tracing: A review. *Science of the Total Environment*, 565, 8–27. <https://doi.org/10.1016/j.scitotenv.2016.04.137>
- Salami, A., Kamara, A.B. & Brixiava, Z. (2010) *Smallholder agriculture in East Africa: Trends, constraints and opportunities*. Tunis: African Development Bank.
- Sanchez, P.A. (2002) Soil fertility and hunger in Africa. *Science*, 295(5562), 2019–2020. <https://doi.org/10.1126/science.1065256>
- Sherriff, S.C., Franks, S.W., Rowan, J.S., Fenton, O. & Ó’Huallacháin, D. (2015) Uncertainty-based assessment of tracer selection, tracer non-conservativeness and multiple solutions in sediment fingerprinting using synthetic and field data. *Journal of Soils and Sediments*, 15(10), 2101–2116. <https://doi.org/10.1007/s11368-015-1123-5>

- Smith, H.G. & Blake, W.H. (2014) Sediment fingerprinting in agricultural catchments: A critical re-examination of source discrimination and data corrections. *Geomorphology*, 204, 177–191. <https://doi.org/10.1016/j.geomorph.2013.08.003>
- Smith, H.G. & Dragovich, D. (2008) Sediment budget analysis of slope-channel coupling and in-channel sediment storage in an upland catchment, southeastern Australia. *Geomorphology*, 101(4), 643–654. <https://doi.org/10.1016/j.geomorph.2008.03.004>
- Smith, H.G., Karam, D.S. & Lennard, A.T. (2018) Evaluating tracer selection for catchment sediment fingerprinting. *Journal of Soils and Sediments*, 18(9), 3005–3019. <https://doi.org/10.1007/s11368-018-1990-7>
- Stock, B.C., Jackson, A.L., Ward, E.J., Parnell, A.C., Phillips, D.L. & Semmens, B.X. (2018) Analyzing mixing systems using a new generation of Bayesian tracer mixing models. *PeerJ*, 6, e5096. <https://doi.org/10.7717/peerj.5096>
- Stock, B.C. & Semmens, B.X. (2016) Unifying error structures in commonly used biotracer mixing models. *Ecology*, 97(10), 2562–2569. <https://doi.org/10.1002/ecy.1517>
- Stock, B.C. & Semmens, B.X. (2017) MixSIAR GUI User Manual v3.1. <https://doi.org/10.5281/zenodo.47719>
- Tengberg, A. & Stocking, M. (1997) *Erosion-induced loss in soil productivity and its impacts on agricultural production and food security*. Harare, Zimbabwe: FAO/AGRITEX Expert Consultation on Integrated Soil Management for Sustainable Agriculture and Food Security in Southern and Eastern Africa, pp. 8–12.
- Ternan, J., Elmes, A., Williams, A. & Hartley, R. (1996) Aggregate stability of soils in central Spain and the role of land management. *Earth Surface Processes and Landforms*, 21(2), 181–193. [https://doi.org/10.1002/\(SICI\)1096-9837\(199602\)21:2<181::AID-ESP622>3.0.CO;2-7](https://doi.org/10.1002/(SICI)1096-9837(199602)21:2<181::AID-ESP622>3.0.CO;2-7)
- Trærup, S.L. & Mertz, O. (2011) Rainfall variability and household coping strategies in northern Tanzania: A motivation for district-level strategies. *Regional Environmental Change*, 11(3), 471–481. <https://doi.org/10.1007/s10113-010-0156-y>
- UNDESA (2017) Population Division – World Population Prospects. In: Division, U.N.P. (Ed.) *The 2017 review*. New York, US: UNDESA.
- Upadhayay, H.R., Bodé, S., Griepentrog, M., Huygens, D., Bajracharya, R. M., Blake, W.H. et al. (2017) Methodological perspectives on the application of compound-specific stable isotope fingerprinting for sediment source apportionment. *Journal of Soils and Sediments*, 17(6), 1537–1553. <https://doi.org/10.1007/s11368-017-1706-4>
- Upadhayay, H.R., Griepentrog, M., Bodé, S., Bajracharya, R.M., Cornelis, W., Collins, A.L. & Boeckx, P. (2020) Catchment-wide variations and biogeochemical time lags in soil fatty acid carbon isotope composition for different land uses: Implications for sediment source classification. *Organic Geochemistry*, 146, 104048. <https://doi.org/10.1016/j.orggeochem.2020.104048>
- Upadhayay, H.R., Smith, H.G., Griepentrog, M., Bodé, S., Bajracharya, R.M., Blake, W. et al. (2018) Community managed forests dominate the catchment sediment cascade in the mid-hills of Nepal: A compound-specific stable isotope analysis. *Science of the Total Environment*, 637, 306–317.
- Valentin, C., Poesen, J. & Li, Y. (2005) Gully erosion: impacts, factors and control. *Catena*, 63(2–3), 132–153. <https://doi.org/10.1016/j.catena.2005.06.001>
- Vanmaercke, M., Poesen, J., Broeckx, J. & Nyssen, J. (2014) Sediment yield in Africa. *Earth-Science Reviews*, 136, 350–368. <https://doi.org/10.1016/j.earscirev.2014.06.004>
- Walling, D.E. (2013) The evolution of sediment source fingerprinting investigations in fluvial systems. *Journal of Soils and Sediments*, 13(10), 1658–1675. <https://doi.org/10.1007/s11368-013-0767-2>
- Walling, D. & Woodward, J. (1995) Tracing sources of suspended sediment in river basins: A case study of the River Culm, Devon, UK. *Marine and Freshwater Research*, 46(1), 327–336. <https://doi.org/10.1071/MF9950327>
- Wilkinson, S.N., Hancock, G.J., Bartley, R., Hawdon, A.A. & Keen, R.J. (2013) Using sediment tracing to assess processes and spatial patterns of erosion in grazed rangelands, Burdekin River basin, Australia. *Agriculture, Ecosystems & Environment*, 180, 90–102. <https://doi.org/10.1016/j.agee.2012.02.002>
- Willis, J.P., Turner, K. & Pritchard, G. (2011) *XRF in the workplace: A guide to practical XRF spectrometry*. Welshpool: PANalytical Australia.
- Wynants, M. (2018) *Pinpointing areas of increased surface erosion risk following land cover changes in the Lake Manyara catchment*. Tanzania: Mendeley Data.
- Wynants, M., Kelly, C., Mtei, K., Munishi, L., Patrick, A., Rabinovich, A. et al. (2019) Drivers of increased soil erosion in East Africa's agro-pastoral systems: Changing interactions between the social, economic and natural domains. *Regional Environmental Change*, 19, 1902–1921.
- Wynants, M., Millward, G., Patrick, A., Taylor, A., Munishi, L., Mtei, K. et al. (2020) Determining tributary sources of increased sedimentation in East-African Rift Lakes. *Science of the Total Environment*, 717, 137266. <https://doi.org/10.1016/j.scitotenv.2020.137266>
- Wynants, M., Patrick, A., Munishi, L., Mtei, K., Bodé, S., Taylor, A. et al. (2021) Soil erosion and sediment transport in Tanzania: Part II – sedimentological evidence of phased land degradation. *Earth Surface Processes and Landforms*. <https://doi.org/10.1002/esp.5218>
- Wynants, M., Solomon, H., Ndakidemi, P. & Blake, W.H. (2018) Pinpointing areas of increased soil erosion risk following land cover change in the Lake Manyara catchment, Tanzania. *International Journal of Applied Earth Observation and Geoinformation*, 71, 1–8. <https://doi.org/10.1016/j.jag.2018.05.008>
- Yu, L. & Oldfield, F. (1993) Quantitative sediment source ascription using magnetic measurements in a reservoir-catchment system near Nijar, S.E. Spain. *Earth Surface Processes and Landforms*, 18(5), 441–454. <https://doi.org/10.1002/esp.3290180506>

SUPPORTING INFORMATION

Additional supporting information may be found in the online version of the article at the publisher's website.

How to cite this article: Wynants, M., Munishi, L., Mtei, K., Bodé, S., Patrick, A., Taylor, A. et al. (2021) Soil erosion and sediment transport in Tanzania: Part I – sediment source tracing in three neighbouring river catchments. *Earth Surface Processes and Landforms*, 46(15), 3096–3111. Available from: <https://doi.org/10.1002/esp.5217>